ADVANCED COMMAND SHAPING ALGORITHM FOR NONLINEAR TOWER CRANE DYNAMICS

D. Blackburn, W. Singhose, J. Kitchen, V. Patrangenaru, J. Lawrence
Georgia Institute of Technology, Atlanta, GA, USA
Singhose@gatech.edu
Tatsuaki Kamoi, Ayako Taura
Tokyo Institute of Technology, Tokyo, Japan

Abstract

Input shaping is an effective method for reducing motion-induced vibration. Input shaping theory is based on linear analysis; however, shaping has proven effective on moderately nonlinear systems. This work investigates the effect of nonlinear crane dynamics on the performance of input shaping. Because typical bridge cranes are driven using Cartesian motions, they behave nearly linearly. The rotational structure of a tower crane makes nonlinearities more apparent. For each system, the nonlinear equations of motion are presented and verified using two portable cranes. The transition from predominantly linear to substantially nonlinear behavior is characterized for the bridge crane. The effectiveness of input shaping on the near–linear bridge crane is explained, and a novel command shaping algorithm is proposed for reducing vibration for the more nonlinear slewing motions of the tower crane.

Introduction

Input shaping is a common method for eliminating vibration, wherein the reference command is altered by convolving it with a series of impulses. Input shaping design is based on the impulse response of linear systems. The nondimensional residual vibration induced by a series of impulses given to a single-mode oscillator is:

$$V = e^{-\zeta\omega t_n}\sqrt{[C(\omega,\zeta)]^2 + [S(\omega,\zeta)]^2} \tag{1}$$

where

$$C(\omega,\zeta) = \sum_{i=1}^{n} A_i e^{\zeta\omega t_i}\cos\left(\omega\sqrt{1-\zeta^2}t_i\right), \quad S(\omega,\zeta) = \sum_{i=1}^{n} A_i e^{\zeta\omega t_i}\sin\left(\omega\sqrt{1-\zeta^2}t_i\right) \tag{2}$$

A_i and t_i are the amplitudes and time locations of the impulses (Singer and Seering [1990]). If the vibration is required to be zero at the modeling frequency, the resulting series of impulses is called a Zero Vibration (ZV) shaper (Smith [1958], Singer and Seering [1990]). For undamped systems, the ZV shaper is given by:

$$\begin{bmatrix} A_i \\ t_i \end{bmatrix} = \begin{bmatrix} 1/2 & 1/2 \\ 0 & T/2 \end{bmatrix}, \quad i = 1,2 \tag{3}$$

where T is the period of oscillation being suppressed. To add robustness to modeling errors, the derivative of vibration with respect to frequency can also be forced to zero at the modeling frequency, yielding the Zero Vibration and Derivative (ZVD) shaper (Singer and Seering [1990]). The ZVD shaper for undamped systems is given by:

$$\begin{bmatrix} A_i \\ t_i \end{bmatrix} = \begin{bmatrix} 1/4 & 1/2 & 1/4 \\ 0 & T/2 & T \end{bmatrix}, \quad i = 1,2,3 \tag{4}$$

These input shapers can be convolved with any reference command to yield a shaped command with vibration-reducing properties. Cranes are ideal candidates for implementing input shaping because they are very lightly damped systems. Input shaping relies on superposition, and because the equations of motion for all cranes are inherently nonlinear, the reliance on superposition is not appropriate for all operating regimes.

This paper investigates two types of cranes, a bridge crane and a tower crane. Nonlinear equations of motion are presented and then verified using a portable bridge crane (Lawrence and Singhose [2005]) at the Georgia Institute of Technology and a portable tower crane (Lawrence et al. [2006]) at the Tokyo Institute of Technology. These equations are linearized, and the transition from predominantly linear to substantially nonlinear behavior is investigated for the bridge crane. The effectiveness of traditional input shaping on bridge cranes is explained. A novel command shaping algorithm is then proposed for dealing with nonlinear tower crane dynamics.

Bridge Crane

System and Modeling

An illustration of a bridge crane is shown in Figure 1. The trolley moves along the bridge in the x direction, and the bridge moves along the runway in the y direction. Thus, the trolley operates in a Cartesian space. If the payload suspension length, L, is held constant, then the equations of motion relating the payload swing angles ϕ and θ to the acceleration of the trolley in the x and y directions are:

$$\begin{aligned} L\ddot{\phi} + L\dot{\theta}^2\cos(\phi)\sin(\phi) + g\sin(\phi)\cos(\theta) &= \ddot{x}\cos(\phi) + \ddot{y}\sin(\phi)\sin(\theta)\,, \\ L\ddot{\theta}\cos(\phi) - 2L\dot{\phi}\dot{\theta}\sin(\phi) + g\sin(\theta) &= -\ddot{y}\cos(\theta)\,. \end{aligned} \tag{5}$$

These equations can be linearized to:

$$\ddot{\phi} = -\frac{g}{L}\phi + \frac{1}{L}\ddot{x}, \quad \ddot{\theta} = -\frac{g}{L}\theta + \frac{1}{L}\ddot{y}. \tag{6}$$

Model Verification

Under normal operation, the payload swing angle is fairly small, thereby causing bridge cranes to behave in a linear manner. To verify the nonlinear equations of motion, a trajectory that induces large swing angles and velocities was chosen to drive both a numerical simulation and the portable bridge crane. Figure 2 shows an overhead view of the simulated and measured payload response. The experimental data and nonlinear simulation show fairly good agreement. Further comparison can be made by graphing the payload swing angles individually. The ϕ profile is shown in Figure 3. The experimental behavior is very close to the nonlinear predictions, and for the extreme motions seen in this example, the nonlinear model shows a clear advantage over the linear model.

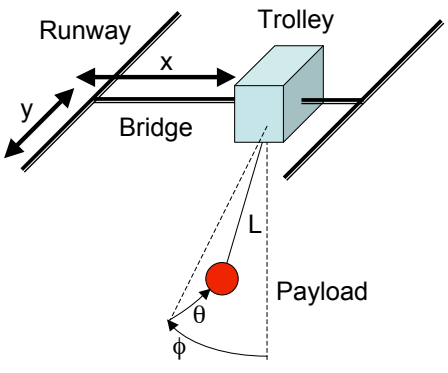

Figure 1. Bridge crane schematic.

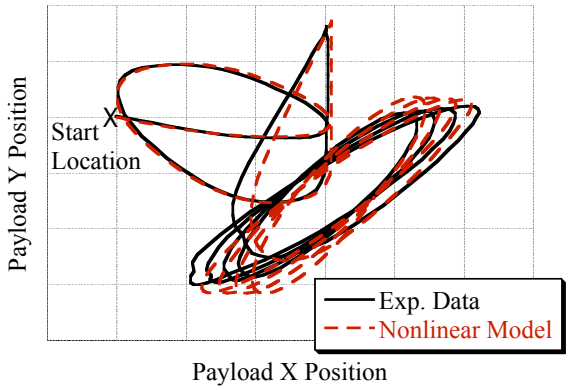

Figure 2. Experimental and nonlinearly simulated payload trajectories.

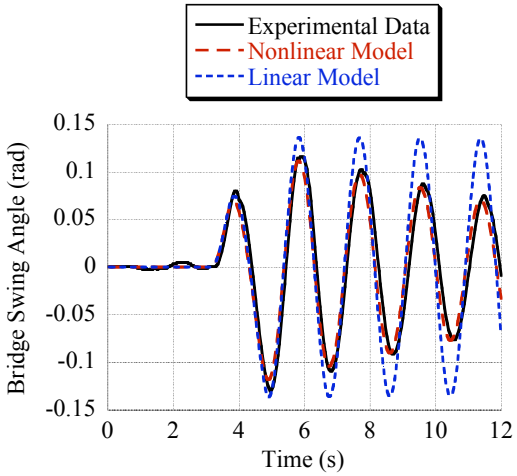

Figure 3. Experimental and simulated trolley swing angle (ϕ).

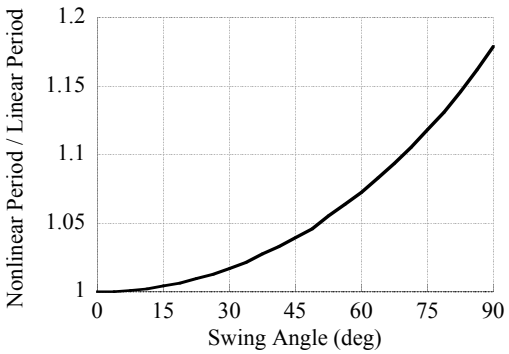

Figure 4. Ratio of nonlinear to linear oscillation periods.

Nonlinear Transition

There are two assumptions that transform the nonlinear crane equations (5) to the linearized model (6). The first assumption is that the payload angular velocity is small: $\left[\dot{\phi},\dot{\theta}\right] \ll 1$. Because these appear as second-order terms in (5), they are neglected. The second assumption is that the angular deflection is small: $[\phi,\theta] \ll 1$. Using the small angle approximations for sine and cosine yields the linearized model, which in turn yields a linear approximation of the oscillation period. As these swing angles increase, the nonlinear period of oscillation changes, as seen in Figure 4. These changes are small. For example, there is only a 5% difference at a swing angle of 50°.

In most real bridge crane operations, large swing angles and velocities are neither safe nor useful. For most reasonable operating regimes, the swing angles and velocities are small enough that there is virtually no difference between the linear and nonlinear models. Because of this, input shaping has been shown to be very effective on bridge cranes (Starr [1985], Singer et al. [1997], Hong and Hong [2004]). In fact, because input shaping suppresses the swing angles, it keeps the crane operating in the linear regime and improves its own effectiveness.

Tower Crane

System and Modeling

An illustration of a tower crane is shown in Figure 5. The trolley slides along the boom in the R direction, and the boom rotates around the mast in the s direction. If the suspension length is constant, then the equations of motion relating the payload swing angles ϕ and θ to the motion of the trolley in the R and s directions are:

$$\begin{gathered} L\ddot{\phi} + L\dot{\theta}^2\cos(\phi)\sin(\phi) + g\sin(\phi)\cos(\theta) = -\ddot{R}\cos(\phi) + R\dot{s}^2\cos(\phi) \\ -R\ddot{s}\sin(\phi)\sin(\theta) - 2\dot{R}\dot{s}\sin(\phi)\sin(\theta) - 2L\dot{s}\dot{\theta}\cos^2(\phi)\cos(\theta) \\ -L\ddot{s}\sin(\theta) + L\dot{s}^2\sin(\phi)\cos^2(\theta)\cos(\phi) \end{gathered} \tag{7}$$

$$\begin{gathered} L\ddot{\theta}\cos(\phi) - 2L\dot{\phi}\dot{\theta}\sin(\phi) + g\sin(\theta) = R\ddot{s}\cos(\theta) + 2\dot{R}\dot{s}\cos(\theta) \\ +2L\dot{s}\dot{\phi}\cos(\phi)\cos(\theta) + L\ddot{s}\sin(\phi)\cos(\theta) + L\dot{s}^2\sin(\theta)\cos(\phi)\cos(\theta) \end{gathered}$$

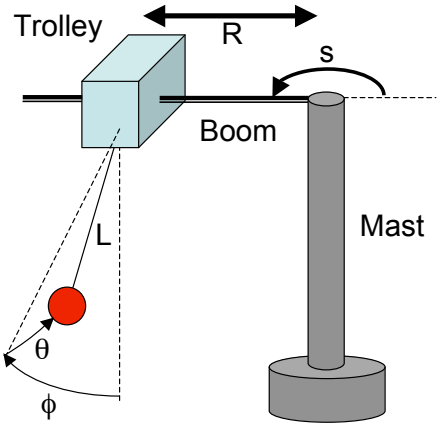

Figure 5. Tower crane schematic.

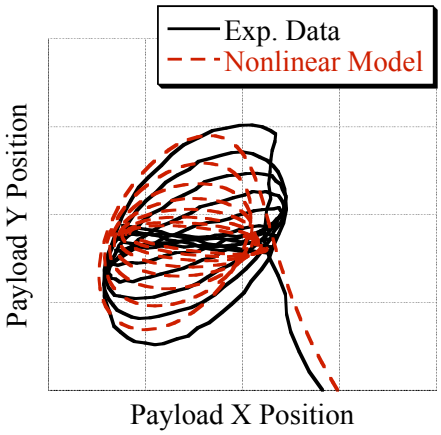

Figure 6. Experimental and nonlinearly simulated payload trajectories.

These can be partially linearized to:

$$\ddot{\phi} = -\frac{g}{L}\phi - \frac{1}{L}\ddot{R}, \quad \ddot{\theta} = -\frac{g}{L}\theta + \frac{R}{L}\ddot{s} \tag{8}$$

These equations are not entirely linear, as indicated by the R/L term. A nominal radius, R_0, could be used to completely linearize the equations, but this is not done here.

Model Verification

Because the tower crane exhibits noticeable nonlinear behavior for nearly all moves, realistic moves were performed and compared with the simulated responses. Figure 6 shows the responses for a combined slew and radial move. As can be seen, the nonlinear simulations predict crane behavior fairly well. The majority of the discrepancy is probably due to nonlinear frictional effects in the trolley drive system that are not included in the nonlinear model. The deflection angles of the payload are well modeled, as shown in Figures 7 and 8. In order to achieve better agreement with the experimental data, a small amount of linear viscous damping was added to the model.

Traditional Input Shapers for Tower Cranes

In order to improve the performance of input shaping, we endeavored to design an input shaper to deal with the specific nonlinearities associated with slewing motions of tower

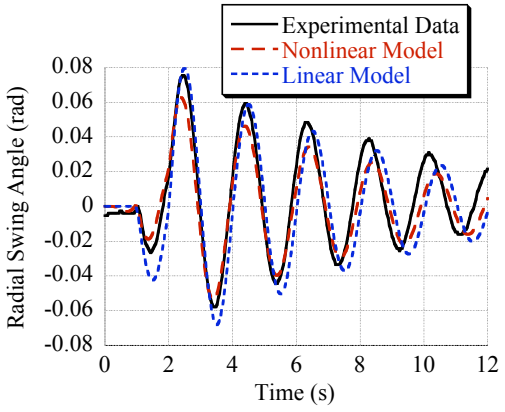

Figure 7. Experimental and simulated radial swing angles (ϕ).

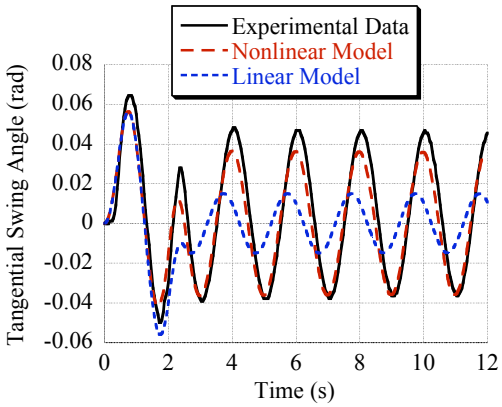

Figure 8. Experimental and simulated tangential swing angles (θ).

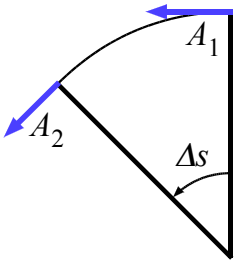

Figure 9. Impulsive effects of ZV shaper.

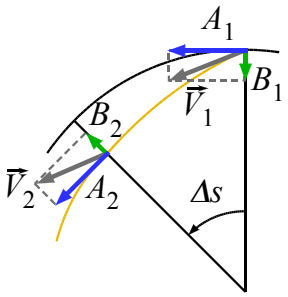

Figure 10. Slewing shaper.

cranes. A traditional ZV shaper convolved with a slewing profile will yield two accelerations in the tangential direction, represented by the arrows in Figure 9. However, due to the rotational nature of the tower crane, these accelerations are not in the same direction. The second acceleration has been rotated through an angle of Δs, which is the change in angle that occurs during the time between the two accelerations. This effect means that the vibration induced by the second acceleration will not perfectly cancel the vibration from the first acceleration.

Nonlinear Slewing Shaper

In order to better cancel the vibration induced by the first acceleration, the second acceleration must act in the same direction. This can be achieved by adding radial accelerations, represented by B_1 and B_2 in Figure 10. The resultant impulsive effects, shown as $\vec{V}_1$ and $\vec{V}_2$, can then be set equal to cancel vibration. A new shaper based on this concept consists of two sets of impulses, one for angular motions, and one for radial motions. This is represented as:

$$\begin{bmatrix} A_i \\ t_i \end{bmatrix} = \begin{bmatrix} \gamma_1 & \gamma_2 \\ 0 & T/2 \end{bmatrix}, \quad \begin{bmatrix} B_i \\ t_i \end{bmatrix} = \begin{bmatrix} -\delta_1 & \delta_1 \\ 0 & T/2 \end{bmatrix} \tag{9}$$

where A_i are the impulse amplitudes in the slewing direction, B_i are those in the radial direction, and t_i are the impulse times. Setting $\vec{V}_1 = \vec{V}_2$ and constraining $\sum A_i = 1$ yields:

$$\gamma_1 + \gamma_2 = 1\,, \quad \delta_1 = \alpha\gamma_1 R_1\,, \quad \gamma_2\left(R_1 - \frac{\delta_1 \ddot{s} t_r}{2}(T - t_r)\right) = \beta\gamma_1 R_1 \tag{10}$$

where R_1 is the starting radial position of the trolley, $\ddot{s}$ is the acceleration of an assumed trapezoidal velocity profile with rise time, $t_r < T/2$, and:

$$\alpha = \frac{1}{[1+\cos(\Delta s)]\cot(\Delta s) + \sin(\Delta s)}\,, \quad \beta = \alpha\frac{1+\cos(\Delta s)}{\sin(\Delta s)}\,, \quad \Delta s = \frac{\gamma_1 \ddot{s} t_r}{2}(T - t_r) \tag{11}$$

Equations (10) and (11) can be solved for the three unknowns, γ_1, γ_2, and δ_1, using a standard nonlinear solver. Once the shapers are determined, they are both convolved with the angular velocity profile to obtain shaped velocity profiles for the radial and slewing directions.

To measure the effectiveness of this new command shaping process, we compared the residual vibration for unshaped, ZV shaped, and ZVD shaped moves against a move using the slewing shaper defined by (9). Representative experimental and simulated results are given in Table 1. In simulation, the slewing shaper performs better than

a ZV shaper, but not as well as the ZVD shaper in terms of vibration suppression. However, the slewing shaper in (9) has the advantage of a shorter rise time than the ZVD shaper. The experimental results show a similar trend, but the slewing shaper does not provide as much radial vibration suppression as predicted. This is most likely due to the hardware being unable to track the command precisely. Note that all of the shaped commands provide large improvements over the unshaped commands.

	Unshaped		**ZV**		**ZVD**		**Slewing Shaper**	
	Sim.	Exp.	Sim.	Exp.	Sim.	Exp.	Sim.	Exp.
Radial Dir.	3.49°	5.33°	0.62°	0.80°	0.18°	0.59°	0.29°	1.30°
Tangential Dir.	7.16°	8.42°	0.42°	0.85°	0.19°	0.65°	0.26°	0.35°

Table 1. Residual vibration amplitude for shaped and unshaped motion.

Conclusions

Nonlinear equations of motion were presented for bridge and tower crane payload motion and verified experimentally. A novel command shaping algorithm was presented for the slewing of tower cranes. The technique is shown to be more effective than traditional input shaping for reducing vibration in the direction of slewing motions. The vector design process used to create the advanced command shaper could also be extended to other input shaping applications that undergo similar transformations during motion.

Acknowledgements

The authors would like to thank Siemens Energy and Automation, the Georgia Tech PURA, and the 21^{st} Century Center of Excellence in Robotics at the Tokyo Institute of Technology for providing equipment and funding for this project.

References

Kyung-Taue Hong and Keum-Shik Hong. Input shaping and VSC of container cranes. In *IEEE Int. Conference on Control App.*, pages 1570–1575, Taipei, Taiwan, 2004.

J. Lawrence, B. Fatkin, W. Singhose, R. Weiss, A. Erb, and U. Glauser. An internet-driven tower crane for dynamics and controls education. In *7th IFAC Symposium on Advances in Control Education*, Madrid, Spain, 2006.

Jason Lawrence and William Singhose. Design of a minicrane for education and research. In *6th International Workshop on Research and Education in Mechatronics*, pages 254–259, Annecy, France, 2005.

N. C. Singer and W. P. Seering. Preshaping command inputs to reduce system vibration. *J. of Dynamic Systems, Measurement, and Control*, 112:76–82, 1990.

Neil Singer, William Singhose, and Eric Kriikku. An input shaping controller enabling cranes to move without sway. In *ANS 7th Topical Meeting on Robotics and Remote Systems*, Augusta, GA, 1997.

O. J. M. Smith. In *Feedback Control Systems*, pages 331–345. McGraw-Hill Book Company, Inc., New York, 1958.

G. P. Starr. Swing-free transport of suspended objects with a path-controlled robot manipulator. *J. of Dynamic Systems, Measurement, and Control*, 107:97–100, 1985.